

Measurement of  $CP$ -violating asymmetries in  $B^0 \rightarrow (\rho\pi)^0$   
using a time-dependent Dalitz plot analysis of the BaBar  
dataset

CKM 2012 Workshop - Cincinnati, Ohio

**Tomonari Miyashita**

on behalf of the BaBar collaboration

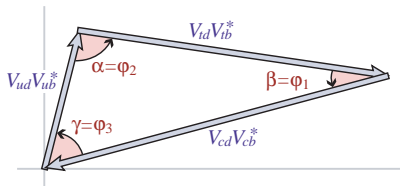
Department of Physics  
Stanford University

Sept 30<sup>th</sup>, 2012



# GENERAL DESCRIPTION

- $B^0 \rightarrow \pi^+ \pi^- \pi^0$  CPV measurement
- Dominated by  $B^0 \rightarrow \rho^\pm \pi^\mp$
- Update of a 2007 BaBar analysis\*
- Extracts information about  $\alpha$ , and other parameters

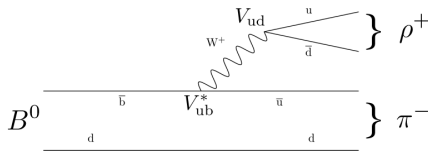


[2011 PDG]

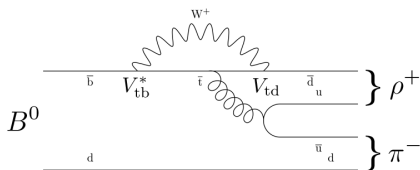
\* Phys. Rev. D 76, 012004 (2007)

# MOTIVATION

- Interference between the tree and penguin modes and decays with and without mixing allows sensitivity to  $\alpha$
- A precision measurement of  $\alpha$  serves to further test the Standard Model through sensitivity to new physics in loops
- The use of a full Dalitz plot analysis reduces ambiguities found in analyses which ignore the interference regions
- Time-Dependent Dalitz Plot  $\rho\pi$  measurement of  $\alpha$  first proposed by Snyder and Quinn\*



Tree Diagram



Penguin Diagram

\* Phys. Rev. D 48, 2139 (1993)

# SUMMARY OF IMPROVEMENTS

- A number of improvements have been made relative to the 2007 analysis:

# SUMMARY OF IMPROVEMENTS

- A number of improvements have been made relative to the 2007 analysis:
  - Increased dataset size by 25% ( $431 \text{ fb}^{-1}$  vs.  $346 \text{ fb}^{-1}$  )

# SUMMARY OF IMPROVEMENTS

- A number of improvements have been made relative to the 2007 analysis:
  - Increased dataset size by 25% (431 fb<sup>-1</sup> vs. 346 fb<sup>-1</sup> )
  - Improved tracking

# SUMMARY OF IMPROVEMENTS

- A number of improvements have been made relative to the 2007 analysis:
  - Increased dataset size by 25% (431 fb<sup>-1</sup> vs. 346 fb<sup>-1</sup> )
  - Improved tracking
  - Improved particle identification

# SUMMARY OF IMPROVEMENTS

- A number of improvements have been made relative to the 2007 analysis:
  - Increased dataset size by 25% (431 fb<sup>-1</sup> vs. 346 fb<sup>-1</sup> )
  - Improved tracking
  - Improved particle identification
  - Reoptimized multivariate discriminator cuts



# SUMMARY OF IMPROVEMENTS

- A number of improvements have been made relative to the 2007 analysis:
  - Increased dataset size by 25% ( $431 \text{ fb}^{-1}$  vs.  $346 \text{ fb}^{-1}$  )
  - Improved tracking
  - Improved particle identification
  - Reoptimized multivariate discriminator cuts
  - Performed more rigorous study of  $\rho$  lineshape systematic uncertainties taking into account correlations between parameters

# SUMMARY OF IMPROVEMENTS

- A number of improvements have been made relative to the 2007 analysis:
  - Increased dataset size by 25% ( $431 \text{ fb}^{-1}$  vs.  $346 \text{ fb}^{-1}$  )
  - Improved tracking
  - Improved particle identification
  - Reoptimized multivariate discriminator cuts
  - Performed more rigorous study of  $\rho$  lineshape systematic uncertainties taking into account correlations between parameters
  - And, importantly, performed robustness studies to assess the reliability with which the true value of  $\alpha$  can be extracted

# SUMMARY OF IMPROVEMENTS

- A number of improvements have been made relative to the 2007 analysis:
  - Increased dataset size by 25% (431 fb<sup>-1</sup> vs. 346 fb<sup>-1</sup> )
  - Improved tracking
  - Improved particle identification
  - Reoptimized multivariate discriminator cuts
  - Performed more rigorous study of  $\rho$  lineshape systematic uncertainties taking into account correlations between parameters
  - And, importantly, performed robustness studies to assess the reliability with which the true value of  $\alpha$  can be extracted

# TIME-DEPENDENT PROBABILITY DISTRIBUTION

$$|\mathcal{A}_{3\pi}^{\pm}(\Delta t)|^2 = \frac{e^{-|\Delta t|/\tau_{B^0}}}{4\tau_{B^0}} \left[ |A_{3\pi}|^2 + |\bar{A}_{3\pi}|^2 \mp (|A_{3\pi}|^2 - |\bar{A}_{3\pi}|^2) \cos(\Delta m_d \Delta t) \pm 2\text{Im} \left[ \frac{q}{p} \bar{A}_{3\pi} A_{3\pi}^* \right] \sin(\Delta m_d \Delta t) \right]$$

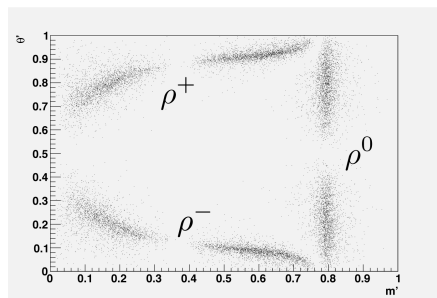
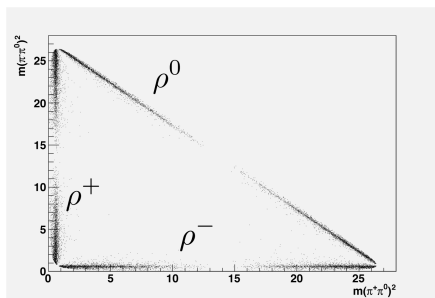
$$A_{3\pi} = f_+ A^+ + f_- A^- + f_0 A^0 \quad \text{for } B^0 \rightarrow \pi^+ \pi^- \pi^0$$

$$\bar{A}_{3\pi} = f_+ \bar{A}^+ + f_- \bar{A}^- + f_0 \bar{A}^0 \quad \text{for } \bar{B}^0 \rightarrow \pi^+ \pi^- \pi^0$$

$$f_{\kappa}(m, \theta_{\kappa}) \propto F_{\rho(770)}(m, \theta_{\kappa}) + a_{\rho'} e^{i\phi_{\rho'}} F_{\rho(1450)}(m, \theta_{\kappa})$$

# EXAMPLE TOY MC DALITZ PLOTS

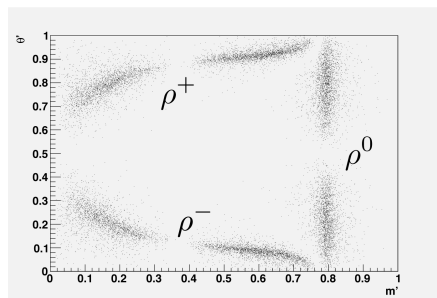
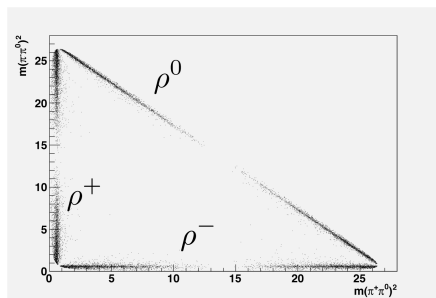
- The Dalitz plot is transformed to cover a unit square before fitting



$\rho\pi$  Toy Dalitz Plot (Left) And Square Dalitz Plot (Right)

# EXAMPLE TOY MC DALITZ PLOTS

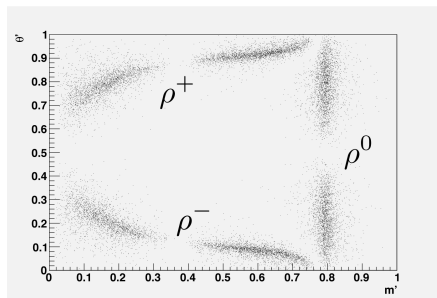
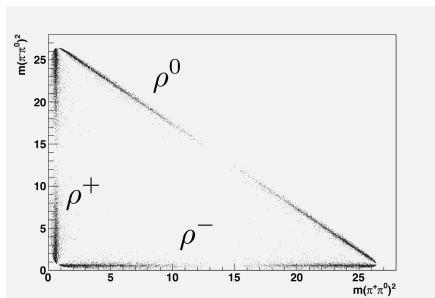
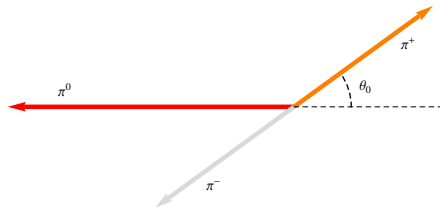
- The Dalitz plot is transformed to cover a unit square before fitting
- $m' \equiv \frac{1}{\pi} \arccos \left( 2 \frac{m_0 - m_0^{\min}}{m_0^{\max} - m_0^{\min}} - 1 \right)$



$\rho\pi$  Toy Dalitz Plot (Left) And Square Dalitz Plot (Right)

# EXAMPLE TOY MC DALITZ PLOTS

- The Dalitz plot is transformed to cover a unit square before fitting
- $m' \equiv \frac{1}{\pi} \arccos \left( 2 \frac{m_0 - m_0^{\min}}{m_0^{\max} - m_0^{\min}} - 1 \right)$
- $\theta' \equiv \frac{1}{\pi} \theta_0$



$\rho\pi$  Toy Dalitz Plot (Left) And Square Dalitz Plot (Right)

# KINEMATIC VARIABLES

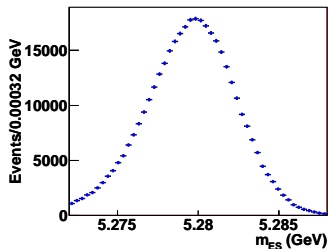
- Loose cuts are applied using beam energy constraints



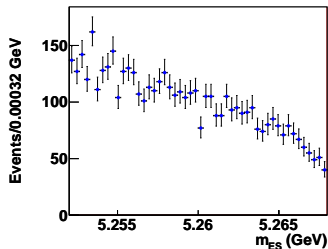
# KINEMATIC VARIABLES

- Loose cuts are applied using beam energy constraints

- $$m_{ES} = \sqrt{\left(\frac{\sqrt{s}}{2}\right)^2 - (p_B^*)^2}$$



$m_{ES}$  In Signal MC



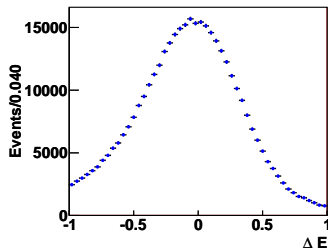
$m_{ES}$  In Data Recorded Below  $B^0\bar{B}^0$  Threshold

# KINEMATIC VARIABLES

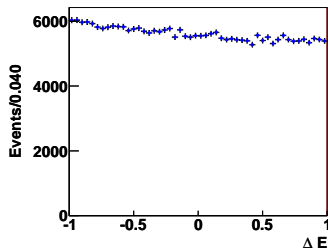
- Loose cuts are applied using beam energy constraints

- $$m_{ES} = \sqrt{\left(\frac{\sqrt{s}}{2}\right)^2 - (p_B^*)^2}$$

- $$\Delta E = E_B^* - \frac{1}{2}\sqrt{s}$$



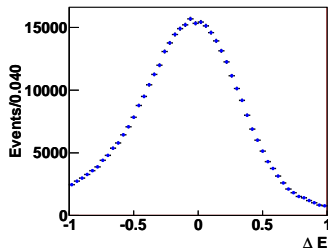
$\Delta E$  In Signal MC



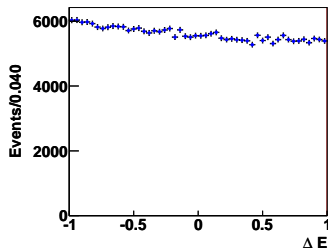
$\Delta E$  In  $m_{ES}$  Sideband Data

# KINEMATIC VARIABLES

- Loose cuts are applied using beam energy constraints
- $m_{ES} = \sqrt{\left(\frac{\sqrt{s}}{2}\right)^2 - (p_B^*)^2}$
- $\Delta E = E_B^* - \frac{1}{2}\sqrt{s}$
- These variables are also included in the fit



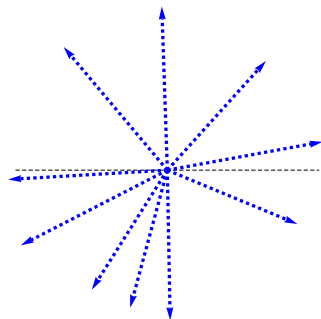
$\Delta E$  In Signal MC



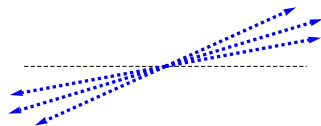
$\Delta E$  In  $m_{ES}$  Sideband Data

# MULTIVARIATE DISCRIMINATOR OPTIMIZATION

- Discriminate signal from continuum ( $q\bar{q}$  where  $q = u, d, s, c$ ) using Neural Net discriminator



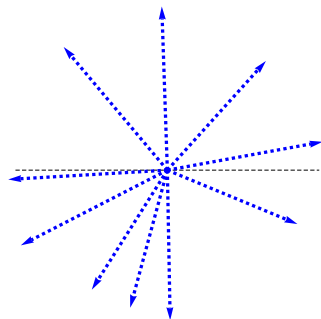
Signal-Like Event Shape



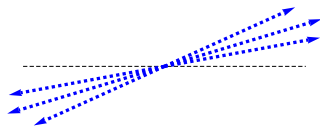
Continuum Event Shape

# MULTIVARIATE DISCRIMINATOR OPTIMIZATION

- Discriminate signal from continuum ( $q\bar{q}$  where  $q = u, d, s, c$ ) using Neural Net discriminator
- 4 Input variables provide sensitivity to event topology



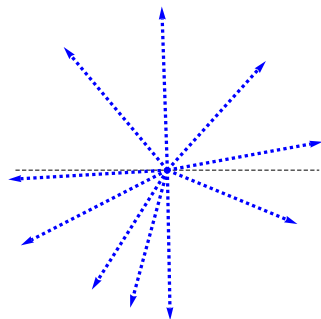
Signal-Like Event Shape



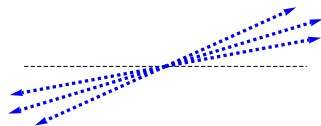
Continuum Event Shape

# MULTIVARIATE DISCRIMINATOR OPTIMIZATION

- Discriminate signal from continuum ( $q\bar{q}$  where  $q = u, d, s, c$ ) using Neural Net discriminator
- 4 Input variables provide sensitivity to event topology
- Trained using:
  - Signal MC with full detector simulation
  - Data collected below the  $B^0\bar{B}^0$  threshold



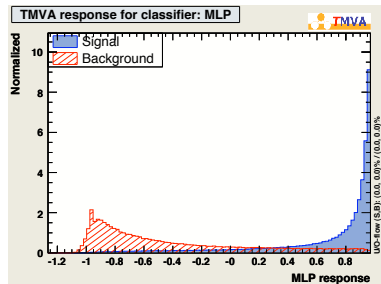
Signal-Like Event Shape



Continuum Event Shape

# MULTIVARIATE DISCRIMINATOR OPTIMIZATION

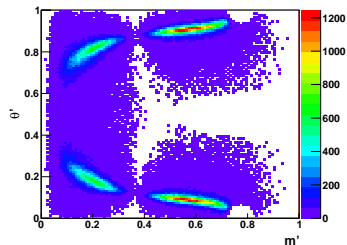
- Discriminate signal from continuum ( $q\bar{q}$  where  $q = u, d, s, c$ ) using Neural Net discriminator
- 4 Input variables provide sensitivity to event topology
- Trained using:
  - Signal MC with full detector simulation
  - Data collected below the  $B^0\bar{B}^0$  threshold
- The NN is used for a loose selection cut and as a variable in the fit



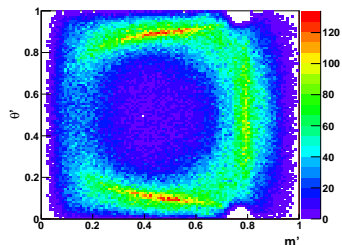
# DATASET OVERVIEW

- Data modeled using four components
  - Correctly reconstructed signal
  - Misreconstructed signal
  - 26  $B$  backgrounds
  - Continuum  $q\bar{q}$  background
- Fixed and initial parameter values are obtained from fits to:
  - Fully simulated MC  
(for signal and  $B$ -bkgs)
  - Data collected below the  $B^0\bar{B}^0$  threshold  
(for continuum)
  - A lower sideband in  $M_{ES}$   
(for continuum)

Correctly Reconstructed Signal MC



$M_{ES}$  Sideband Data





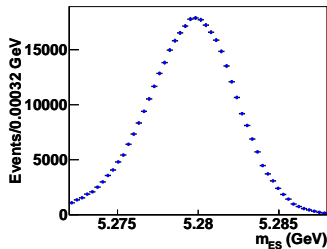
# FITTING

- Data is fit using a multi-dimensional extended maximum likelihood approach with 6 input variables:

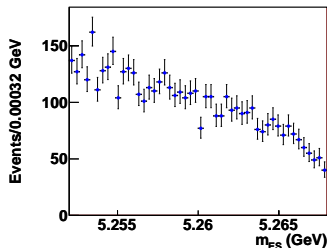
# FITTING

- Data is fit using a multi-dimensional extended maximum likelihood approach with 6 input variables:
  - $m_{ES}$

$m_{ES}$  In Signal MC



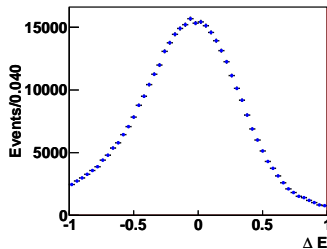
$m_{ES}$  In Below  $B^0\bar{B}^0$  Threshold Data



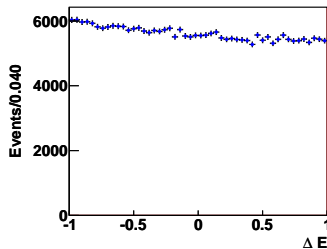
# FITTING

- Data is fit using a multi-dimensional extended maximum likelihood approach with 6 input variables:
  - $m_{ES}$ ,  $\Delta E$

$\Delta E$  In Signal MC



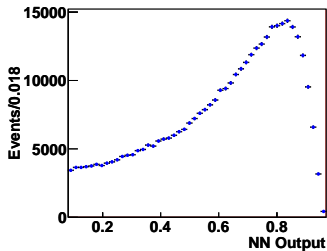
$\Delta E$  In Sideband Data



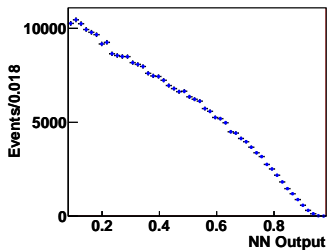
# FITTING

- Data is fit using a multi-dimensional extended maximum likelihood approach with 6 input variables:
  - $m_{ES}$ ,  $\Delta E$ , NN output

$NN_{out}$  In Signal MC

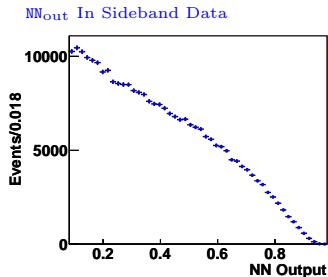
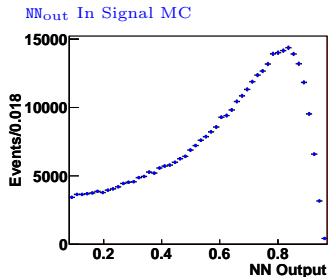


$NN_{out}$  In Sideband Data



# FITTING

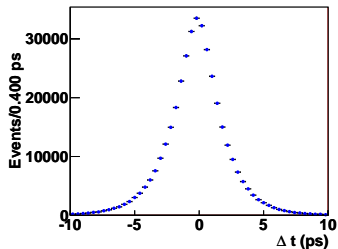
- Data is fit using a multi-dimensional extended maximum likelihood approach with 6 input variables:
  - $m_{ES}$ ,  $\Delta E$ , NN output
  - Time-Dependent SDP:



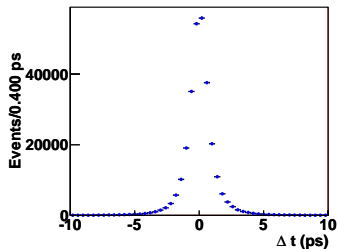
# FITTING

- Data is fit using a multi-dimensional extended maximum likelihood approach with 6 input variables:
  - $m_{ES}$ ,  $\Delta E$ , NN output
  - Time-Dependent SDP:  $\Delta t$

$\Delta t$  In Signal MC



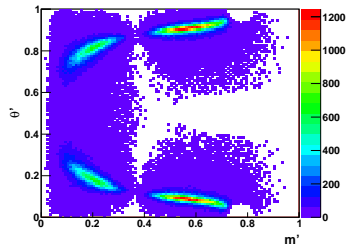
$\Delta t$  In Sideband Data



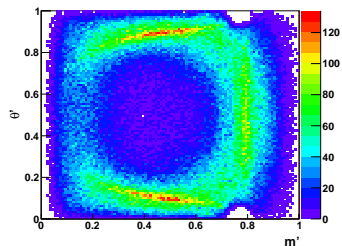
# FITTING

- Data is fit using a multi-dimensional extended maximum likelihood approach with 6 input variables:
  - $m_{ES}$ ,  $\Delta E$ , NN output
  - Time-Dependent SDP:  $\Delta t$ ,  $(m', \theta')$

Signal MC



$M_{ES}$  Sideband Data



# PARAMETERIZATION

- There are several possible parameterizations for the decay probability
- Each parameterization has advantages and drawbacks



# PARAMETERIZATION

- There are several possible parameterizations for the decay probability
- Each parameterization has advantages and drawbacks
  - Using magnitudes and phases (10 free parameters) leads to problems with non-gaussian errors when magnitudes are small

# PARAMETERIZATION

- There are several possible parameterizations for the decay probability
- Each parameterization has advantages and drawbacks
  - Using magnitudes and phases (10 free parameters) leads to problems with non-gaussian errors when magnitudes are small
  - Using real and imaginary parts of amplitudes leads to ambiguous solutions and difficulty in extracting physics parameters like  $\alpha$

# PARAMETERIZATION

- There are several possible parameterizations for the decay probability
- Each parameterization has advantages and drawbacks
  - Using magnitudes and phases (10 free parameters) leads to problems with non-gaussian errors when magnitudes are small
  - Using real and imaginary parts of amplitudes leads to ambiguous solutions and difficulty in extracting physics parameters like  $\alpha$
  - Using a more sophisticated parameterization (26 free parameters) reduces ambiguities in the solution and provides gaussian errors, but solutions may be unphysical

# PARAMETERIZATION

- There are several possible parameterizations for the decay probability
- Each parameterization has advantages and drawbacks
  - Using magnitudes and phases (10 free parameters) leads to problems with non-gaussian errors when magnitudes are small
  - Using real and imaginary parts of amplitudes leads to ambiguous solutions and difficulty in extracting physics parameters like  $\alpha$
  - Using a more sophisticated parameterization (26 free parameters) reduces ambiguities in the solution and provides gaussian errors, but solutions may be unphysical
- Ultimately, it was determined that the third parameterization (with 26 free parameters) is the most practical option

# $U/I$ PARAMETERIZATION I

- In our parameterization, 26 “ $U$  and  $I$ ” parameters are calculated from the  $\rho$  resonance amplitudes:

$$\begin{aligned}U_{\kappa}^{\pm} &= |A^{\kappa}|^2 \pm |\bar{A}^{\kappa}|^2 \\U_{\kappa\sigma}^{\pm, \text{Re(Im)}} &= \text{Re(Im)} \left[ A^{\kappa} A^{\sigma*} \pm \bar{A}^{\kappa} \bar{A}^{\sigma*} \right] \\I_{\kappa} &= \text{Im} \left[ \bar{A}^{\kappa} A^{\kappa*} \right] \\I_{\kappa\sigma}^{\text{Re}} &= \text{Re} \left[ \bar{A}^{\kappa} A^{\sigma*} - \bar{A}^{\sigma} A^{\kappa*} \right] \\I_{\kappa\sigma}^{\text{Im}} &= \text{Im} \left[ \bar{A}^{\kappa} A^{\sigma*} + \bar{A}^{\sigma} A^{\kappa*} \right]\end{aligned}$$

# $U/I$ PARAMETERIZATION II

- The time-dependent probability distribution may then be expressed in terms of these parameters as

$$|\mathcal{A}_{3\pi}^{\pm}(\Delta t)|^2 = \frac{e^{-|\Delta t|/\tau_{B^0}}}{4\tau_{B^0}} \left[ |A_{3\pi}|^2 + |\bar{A}_{3\pi}|^2 \mp (|A_{3\pi}|^2 - |\bar{A}_{3\pi}|^2) \cos(\Delta m_d \Delta t) \pm 2\text{Im} \left[ \frac{q}{p} \bar{A}_{3\pi} A_{3\pi}^* \right] \sin(\Delta m_d \Delta t) \right]$$

- where

$$|A_{3\pi}|^2 \pm |\bar{A}_{3\pi}|^2 = \sum_{\kappa \in \{+, -, 0\}} |f_{\kappa}|^2 U_{\kappa}^{\pm} + 2 \sum_{\kappa < \sigma \in \{+, -, 0\}} \left( \text{Re} [f_{\kappa} f_{\sigma}^*] U_{\kappa\sigma}^{\pm, \text{Re}} - \text{Im} [f_{\kappa} f_{\sigma}^*] U_{\kappa\sigma}^{\pm, \text{Im}} \right)$$
$$\text{Im} \left[ \frac{q}{p} \bar{A}_{3\pi} A_{3\pi}^* \right] = \sum_{\kappa \in \{+, -, 0\}} |f_{\kappa}|^2 I_{\kappa} + \sum_{\kappa < \sigma \in \{+, -, 0\}} \left( \text{Re} [f_{\kappa} f_{\sigma}^*] I_{\kappa\sigma}^{\text{Im}} + \text{Im} [f_{\kappa} f_{\sigma}^*] I_{\kappa\sigma}^{\text{Re}} \right)$$

# SYSTEMATIC STUDIES - THE $\rho(1700)$

- Ideally, the systematic associated with omitting the  $\rho(1700)$  from our nominal fit would be calculated simply by fitting our full dataset with and without the  $\rho(1700)$ 
  - This does not properly account for uncertainties arising from the fact that we only have one dataset

# SYSTEMATIC STUDIES - THE $\rho(1700)$

- Ideally, the systematic associated with omitting the  $\rho(1700)$  from our nominal fit would be calculated simply by fitting our full dataset with and without the  $\rho(1700)$ 
  - This does not properly account for uncertainties arising from the fact that we only have one dataset
- In order to estimate an uncertainty on the changes in the fit parameters when including the  $\rho(1700)$ , we use the bootstrap method



# SYSTEMATIC STUDIES - THE $\rho(1700)$

- Ideally, the systematic associated with omitting the  $\rho(1700)$  from our nominal fit would be calculated simply by fitting our full dataset with and without the  $\rho(1700)$ 
  - This does not properly account for uncertainties arising from the fact that we only have one dataset
- In order to estimate an uncertainty on the changes in the fit parameters when including the  $\rho(1700)$ , we use the bootstrap method
- The bootstrap technique allows one to estimate the uncertainty on parameters calculated from a single dataset

# SYSTEMATIC STUDIES - THE $\rho(1700)$

- Ideally, the systematic associated with omitting the  $\rho(1700)$  from our nominal fit would be calculated simply by fitting our full dataset with and without the  $\rho(1700)$ 
  - This does not properly account for uncertainties arising from the fact that we only have one dataset
- In order to estimate an uncertainty on the changes in the fit parameters when including the  $\rho(1700)$ , we use the bootstrap method
- The bootstrap technique allows one to estimate the uncertainty on parameters calculated from a single dataset
- This is done by sampling with replacement from the original dataset to generate N “bootstrapped” datasets

# SYSTEMATIC STUDIES - THE $\rho(1700)$

- Ideally, the systematic associated with omitting the  $\rho(1700)$  from our nominal fit would be calculated simply by fitting our full dataset with and without the  $\rho(1700)$ 
  - This does not properly account for uncertainties arising from the fact that we only have one dataset
- In order to estimate an uncertainty on the changes in the fit parameters when including the  $\rho(1700)$ , we use the bootstrap method
- The bootstrap technique allows one to estimate the uncertainty on parameters calculated from a single dataset
- This is done by sampling with replacement from the original dataset to generate N “bootstrapped” datasets
- If one fits to each dataset, then the covariances of the fit variables across all the “bootstrapped” datasets provide an estimate of the variables’ uncertainties

# SYSTEMATIC STUDIES - THE $\rho(1700)$ II

- Bootstrapped estimate of the uncertainty on changes in  $U/I$  parameters between fits with and without the  $\rho(1700)$ , and the ratio of the mean change in the  $U/I$  parameters across all bootstrapped fits to their estimated uncertainties.

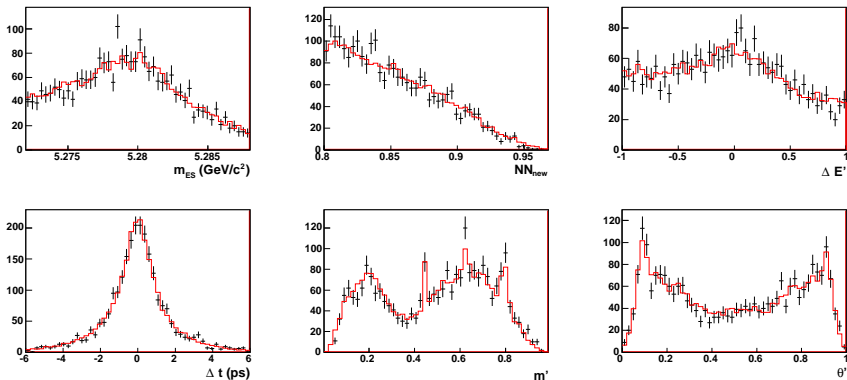
Parameter	$\sigma_{\Delta U}$	$\langle \Delta U \rangle / \sigma_{\Delta U}$	Parameter	$\sigma_{\Delta U}$	$\langle \Delta U \rangle / \sigma_{\Delta U}$
$I_0$	0.020	-0.36	$U_{-0}^{+, \text{Re}}$	0.17	-0.8
$I_-$	0.022	0.41	$U_-^-$	0.034	0.19
$I_{-0}^{\text{Im}}$	0.42	-0.7	$U_-^+$	0.05	0.15
$I_{-0}^{\text{Re}}$	0.7	0.28	$U_{+0}^{-, \text{Im}}$	0.44	-0.10
$I_+$	0.023	0.18	$U_{+0}^{-, \text{Re}}$	0.36	0.5
$I_{+0}^{\text{Im}}$	0.42	-0.11	$U_{+0}^{+, \text{Im}}$	0.16	0.5
$I_{+0}^{\text{Re}}$	0.7	0.26	$U_{+0}^{+, \text{Re}}$	0.17	0.05
$I_{+-}^{\text{Im}}$	0.9	-1.0	$U_{+-}^{-, \text{Im}}$	0.8	-0.27
$I_{+-}^{\text{Re}}$	0.9	-0.6	$U_{+-}^{-, \text{Re}}$	0.7	0.15
$U_0^-$	0.029	0.29	$U_{+-}^{+, \text{Im}}$	0.25	-0.22
$U_0^+$	0.017	0.5	$U_{+-}^{+, \text{Re}}$	0.28	-0.21
$U_{-0}^{-, \text{Im}}$	0.5	0.8	$U_{+}^-$	0.06	-0.5
$U_{-0}^{-, \text{Re}}$	0.34	0.5			
$U_{-0}^{+, \text{Im}}$	0.21	-0.8			

# SYSTEMATIC STUDIES - THE $\rho(1700)$ III

- The changes in the fit parameters are small relative to the uncertainty on the fit parameters and the estimated uncertainty on the changes in the fit parameters
- Therefore, we choose the covariance matrix of the bootstrapped changes as our systematic covariance matrix and don't correct for any bias
- A similar bootstrapped systematic study is performed to assess the systematic uncertainty associated with a non-resonant component, and the effect is found to be even smaller than for the  $\rho(1700)$  systematic

# FINAL FIT RESULTS BABAR PRELIMINARY

- From an on-resonance dataset containing 53,084 events, our multi-dimensional fit extracts  $2,940 \pm 100$  signal events and  $46,750 \pm 220$  continuum events.
- Goodness of fit is demonstrated by the figure below, which contains overlaid plots of the data used in the final fit and parameterized MC generated using the results of the final fit and equivalent to 10 times the data sample.
- The signal component of these plots is enhanced by a tight cut on the NN variable.



Agreement between data (points with error bars) and fit results (red)



# FINAL $U/I$ FIT RESULTS BABAR PRELIMINARY

- The  $U$  and  $I$  parameter values extracted from our final fit are given in the tables below along with stat and syst errors:

$$\langle \sigma_{\text{stat}}^{\text{new}} / \sigma_{\text{stat}}^{2007} \rangle = 0.47$$

Parameter	Final Fit Value
$I_0$	$-0.042 \pm 0.038 \pm 0.022$
$I_-$	$-0.00 \pm 0.06 \pm 0.03$
$I_{-0}^{\text{Im}}$	$-0.61 \pm 0.43 \pm 0.46$
$I_{-0}^{\text{Re}}$	$0.4 \pm 0.6 \pm 0.8$
$I_+$	$0.05 \pm 0.06 \pm 0.03$
$I_{+0}^{\text{Im}}$	$-0.04 \pm 0.36 \pm 0.43$
$I_{+0}^{\text{Re}}$	$0.5 \pm 0.5 \pm 0.7$
$I_{+-}^{\text{Im}}$	$-0.5 \pm 0.7 \pm 0.9$
$I_{+-}^{\text{Re}}$	$-0.6 \pm 0.8 \pm 1.0$
$U_0^-$	$0.04 \pm 0.05 \pm 0.03$
$U_0^+$	$0.225 \pm 0.030 \pm 0.020$
$U_{-0}^{-,\text{Im}}$	$0.53 \pm 0.44 \pm 0.52$
$U_{-0}^{-,\text{Re}}$	$0.49 \pm 0.35 \pm 0.37$
$U_{-0}^{+,\text{Im}}$	$-0.39 \pm 0.20 \pm 0.24$

Parameter	Final Fit Value
$U_{-0}^{+,\text{Re}}$	$-0.05 \pm 0.17 \pm 0.18$
$U_-^-$	$-0.27 \pm 0.10 \pm 0.06$
$U_-^+$	$1.22 \pm 0.07 \pm 0.05$
$U_{+0}^{-,\text{Im}}$	$0.10 \pm 0.29 \pm 0.45$
$U_{+0}^{-,\text{Re}}$	$0.30 \pm 0.32 \pm 0.38$
$U_{+0}^{+,\text{Im}}$	$0.41 \pm 0.16 \pm 0.17$
$U_{+0}^{+,\text{Re}}$	$0.01 \pm 0.15 \pm 0.19$
$U_{+-}^{-,\text{Im}}$	$1.1 \pm 0.5 \pm 0.8$
$U_{+-}^{-,\text{Re}}$	$-0.5 \pm 0.5 \pm 0.8$
$U_{+-}^{+,\text{Im}}$	$-0.07 \pm 0.26 \pm 0.26$
$U_{+-}^{+,\text{Re}}$	$-0.19 \pm 0.25 \pm 0.33$
$U_+^-$	$0.25 \pm 0.09 \pm 0.07$

# $U/I$ ROBUSTNESS STUDY I

- In order to judge the robustness with which the correct values of  $U$  and  $I$  parameters can be extracted by the fit framework, a series of studies were performed
- We perform fits to 25 toy MC datasets generated with expected “on-resonance” dataset statistics and a shared set of known parameter values (with  $\alpha = 89^\circ$ ), but different random seeds
- $U$  and  $I$  parameter values are extracted in fits to each of these datasets and their agreement with the generated values is assessed



# U/I ROBUSTNESS STUDY II

- U/I Robustness Study Results:

$$\langle \text{RMS } \# \sigma \text{ Diff From Gen Val} \rangle = 1.17$$

$$\langle \text{Avg } \# \sigma \text{ Diff From Gen Val} \rangle = 0.04$$

Param	RMS # $\sigma$ Diff From Gen Val	Avg # $\sigma$ Diff From Gen Val
$I_0$	1.05	0.27
$I_-$	1.21	0.18
$I_{-0}^{\text{Im}}$	1.24	-0.10
$I_{-0}^{\text{Re}}$	1.29	0.09
$I_+$	1.01	-0.17
$I_{+0}^{\text{Im}}$	1.30	0.17
$I_{+0}^{\text{Re}}$	1.31	0.22
$I_{+-}^{\text{Im}}$	1.03	-0.08
$I_{+-}^{\text{Re}}$	1.09	-0.07
$U_0^-$	1.14	-0.12
$U_0^+$	1.09	0.29
$U_{-0}^{-,\text{Im}}$	1.62	0.19
$U_{-0}^{-,\text{Re}}$	1.29	-0.02
$U_{-0}^{+,\text{Im}}$	1.50	-0.62

Param	RMS # $\sigma$ Diff From Gen Val	Avg # $\sigma$ Diff From Gen Val
$U_{-0}^{+,\text{Re}}$	1.18	0.44
$U_-^-$	1.06	0.01
$U_-^+$	0.95	0.12
$U_{+0}^{-,\text{Im}}$	1.49	0.20
$U_{+0}^{-,\text{Re}}$	0.82	-0.08
$U_{+0}^{+,\text{Im}}$	1.41	-0.13
$U_{+0}^{+,\text{Re}}$	0.93	-0.03
$U_{+-}^{-,\text{Im}}$	1.08	0.33
$U_{+-}^{-,\text{Re}}$	1.25	-0.29
$U_{+-}^{+,\text{Im}}$	1.13	-0.14
$U_{+-}^{+,\text{Re}}$	1.12	0.44
$U_+^-$	0.88	0.08

# QUASI-TWO-BODY FIT RESULTS I

- The  $U$  and  $I$  parameters extracted from our final fit may be used to calculate the values of quasi-two-body (Q2B) parameters often used in  $CP$ -violation analyses:

$$f_{Q_{\text{tag}}^{\rho^{\pm}\pi^{\mp}}}(\Delta t) = (1 \pm \mathcal{A}_{\rho\pi}) \frac{e^{-|\Delta t|/\tau}}{4\tau} \\ \times [1 + Q_{\text{tag}}(S \pm \Delta S) \sin(\Delta m_d \Delta t) \\ - Q_{\text{tag}}(C \pm \Delta C) \cos(\Delta m_d \Delta t)].$$

with

$$\mathcal{A}_{\rho\pi} = \frac{U_+^+ - U_-^+}{U_+^+ + U_-^+},$$

and

$$c = (c^+ + c^-)/2, \\ \Delta c = (c^+ - c^-)/2, \\ s = (s^+ + s^-)/2, \\ \Delta s = (s^+ - s^-)/2.$$

where

$$c^+ = \frac{U_+^-}{U_+^+}, \quad c^- = \frac{U_-^-}{U_-^+}, \quad s^+ = \frac{2I_+}{U_+^+}, \quad s^- = \frac{2I_-}{U_-^+},$$

# QUASI-TWO-BODY FIT RESULTS II

- We can also use our fit results to extract the Q2B  $B^0 \rightarrow \rho^0 \pi^0$   $CP$ -violation parameters and decay fraction:

$$c_{00} = \frac{U_0^-}{U_0^+},$$
$$s_{00} = \frac{2I_0}{U_0^+},$$
$$f_{00} = \frac{U_0^+}{U_+^+ + U_-^+ + U_0^+}.$$

- All eight of these Q2B parameters are extracted in a  $\chi^2$  minimization using the full stat+syst covariance matrix for the relevant  $U$  and  $I$  parameters:

Param	Value	$\sigma_{\text{stat}}$	$\sigma_{\text{syst}}$
$\mathcal{A}_{\rho\pi}$	-0.100	0.029	0.021
$\mathcal{C}$	0.016	0.059	0.036
$\Delta\mathcal{C}$	0.234	0.061	0.048
$\mathcal{S}$	0.053	0.081	0.034
$\Delta\mathcal{S}$	0.054	0.082	0.039
$\mathcal{C}_{00}$	0.19	0.23	0.15
$\mathcal{S}_{00}$	-0.37	0.34	0.20
$f_{00}$	0.092	0.011	0.008

BaBar Preliminary

# QUASI-TWO-BODY FIT RESULTS III

- The parameters  $\mathcal{A}_{\rho\pi}$  and  $\mathcal{C}$  can be transformed into the direct  $CP$ -violation parameters  $\mathcal{A}_{\rho\pi}^{+-}$  and  $\mathcal{A}_{\rho\pi}^{-+}$  where

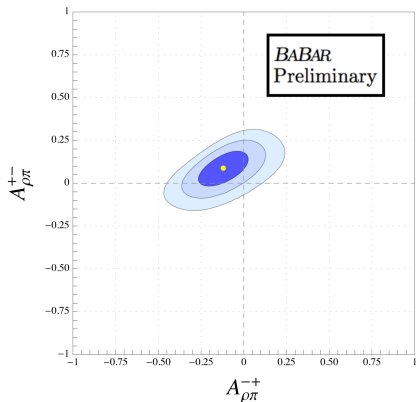
$$\mathcal{A}_{\rho\pi}^{+-} \equiv \frac{\Gamma(\bar{B}^0 \rightarrow \rho^- \pi^+) - \Gamma(B^0 \rightarrow \rho^+ \pi^-)}{\Gamma(\bar{B}^0 \rightarrow \rho^- \pi^+) + \Gamma(B^0 \rightarrow \rho^+ \pi^-)} = -\frac{\mathcal{A}_{\rho\pi} + \mathcal{C} + \mathcal{A}_{\rho\pi} \Delta\mathcal{C}}{1 + \Delta\mathcal{C} + \mathcal{A}_{\rho\pi} \mathcal{C}},$$
$$\mathcal{A}_{\rho\pi}^{-+} \equiv \frac{\Gamma(\bar{B}^0 \rightarrow \rho^+ \pi^-) - \Gamma(B^0 \rightarrow \rho^- \pi^+)}{\Gamma(\bar{B}^0 \rightarrow \rho^+ \pi^-) + \Gamma(B^0 \rightarrow \rho^- \pi^+)} = \frac{\mathcal{A}_{\rho\pi} - \mathcal{C} - \mathcal{A}_{\rho\pi} \Delta\mathcal{C}}{1 - \Delta\mathcal{C} - \mathcal{A}_{\rho\pi} \mathcal{C}}.$$

- These parameters are extracted in a 2-dimensional likelihood scan yielding:

$$\mathcal{A}_{\rho\pi}^{+-} = 0.09_{-0.06}^{+0.05} \pm 0.04,$$
$$\mathcal{A}_{\rho\pi}^{-+} = -0.12 \pm 0.08_{-0.05}^{+0.04}.$$

# QUASI-TWO-BODY FIT RESULTS IV

- In the 2D scan, the origin, corresponding to no direct  $CP$  violation, lies on the 96.0% confidence-level contour ( $\Delta\chi^2 = 6.42$ )



# QUASI-TWO-BODY ROBUSTNESS STUDY

- We assess the robustness with which the Q2B parameters are extracted using the same toy MC as used for the  $U/I$  robustness study
- Q2B Robustness Study Results:

Param	$\sqrt{\text{Variance}} / \langle \sigma \rangle$	Avg # $\sigma$ Diff From Gen Val
$\mathcal{A}_{\rho\pi}$	0.94	-0.13
$\mathcal{C}$	1.15	0.06
$\Delta\mathcal{C}$	0.94	0.04
$\mathcal{S}$	1.11	0.03
$\Delta\mathcal{S}$	1.02	-0.20
$\mathcal{C}_{00}$	1.15	-0.10
$\mathcal{S}_{00}$	1.13	0.23
$f_{00}$	1.08	0.28

# $\alpha$ SCAN TECHNIQUE

- Information about the unitarity triangle angle  $\alpha$  is extracted in a likelihood scan based on our final  $U/I$  fit results and full stat+syst covariance matrix
- Perform a  $\chi^2$  minimization at each value of  $\alpha$  from (0 – 180) degrees using

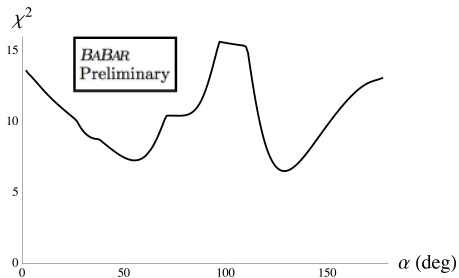
$$\chi_{\alpha \text{ scan}}^2 = \left[ V^{\text{data}} - V^{\text{scan}} \right]^T (C^{\text{data}})^{-1} \left[ V^{\text{data}} - V^{\text{scan}} \right]$$

- The variables that float in these fits are actually the tree and penguin amplitudes which are related to the  $\rho$  amplitudes by:

$$\begin{aligned} A^+ &= T^+ e^{-i\alpha} + P^+ \\ A^- &= T^- e^{-i\alpha} + P^- \\ A^0 &= T^0 e^{-i\alpha} + P^0 \\ \bar{A}^+ &= T^- e^{+i\alpha} + P^- \\ \bar{A}^- &= T^+ e^{+i\alpha} + P^+ \\ \bar{A}^0 &= T^0 e^{+i\alpha} + P^0 \end{aligned}$$

# FINAL FIT $\alpha$ SCAN RESULTS

- $\alpha$  scan results including stat+syst uncertainties:

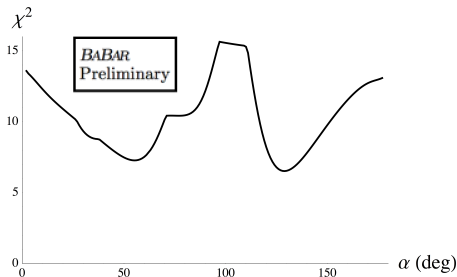


$\alpha$  Scan  $\chi^2$  Distribution

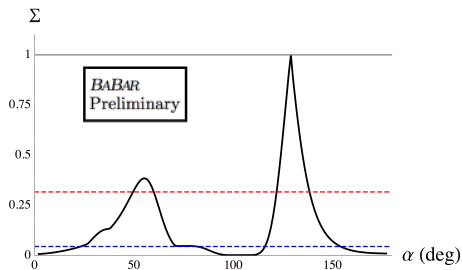


# FINAL FIT $\alpha$ SCAN RESULTS

- $\alpha$  scan results including stat+syst uncertainties:
- ( $\Sigma$  is calculated as the integral of a  $\chi^2$  distribution with 1 degree of freedom from  $\Delta\chi^2$  to  $\infty$ )
- $\Sigma$  corresponds to what is commonly referred to as “1 – C.L.”



$\alpha$  Scan  $\chi^2$  Distribution



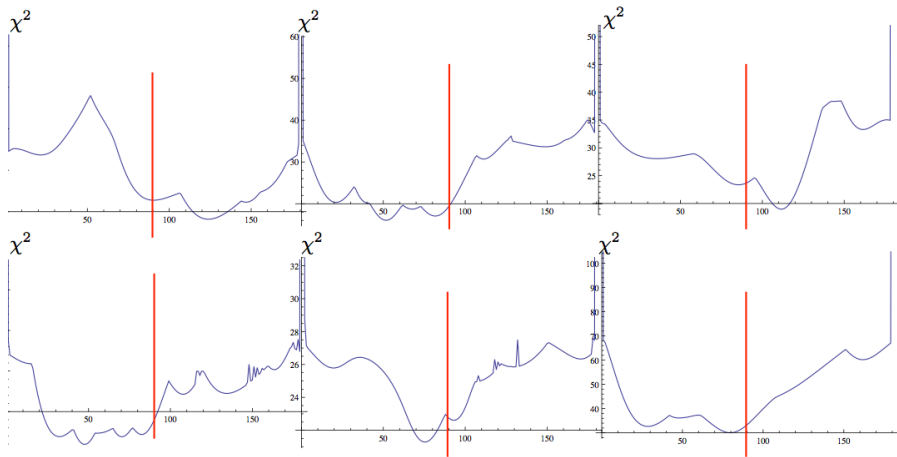
$\alpha$  Scan  $\Sigma$  Distribution  
(See robustness studies for interpretation)

# $\alpha$ SCAN ROBUSTNESS STUDIES I

- In order to judge the robustness with which the correct value of  $\alpha$  can be extracted by the fit framework, a series of studies were performed
- We perform  $\alpha$  scans using the 25 toy MC datasets from the previous robustness studies and assess the robustness with which the generated value of  $\alpha$  ( $89^\circ$ ) is extracted

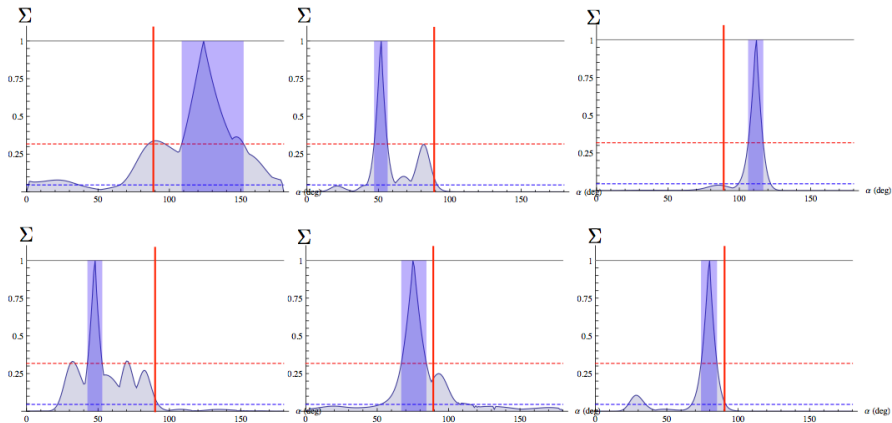
# $\alpha$ SCAN ROBUSTNESS STUDIES II

- Example  $\alpha$  Scan  $\chi^2$  Distributions ( $\alpha_{\text{gen}} = 89^\circ$ )



# $\alpha$ SCAN ROBUSTNESS STUDIES III

● Example  $\alpha$  Scan  $\Sigma$  Distributions ( $\alpha_{\text{gen}} = 89^\circ$ )

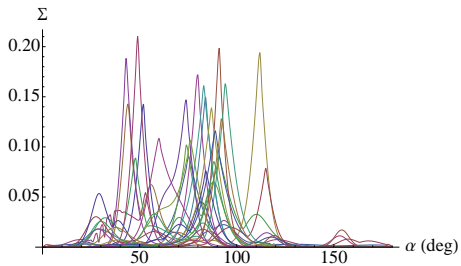


# $\alpha$ SCAN ROBUSTNESS STUDIES IV

$\alpha$ Scan Peak	Mean Error	# $\sigma$ Between Gen and Fit Peaks
43	4.6	-9.0
44	5.0	-8.5
48	5.2	-8.2
49	4.6	-8.7
52	4.7	-8.2
53	12.8	-7.2
60	10.9	-2.1
74	6.5	-2.1
74	9.0	-2.9
75	8.8	-1.5
76	12.6	-1.7
80	5.6	-1.7
83	6.9	-0.94
84	5.9	-0.89
84	6.7	-0.72
87	7.1	-0.29
88	6.7	-0.14
89	8.4	0
91	9.2	0.22
91	4.5	0.43
92	6.9	0.48
94	6.3	0.89
112	5.3	3.9
115	5.4	4.6
124	21.7	2.3

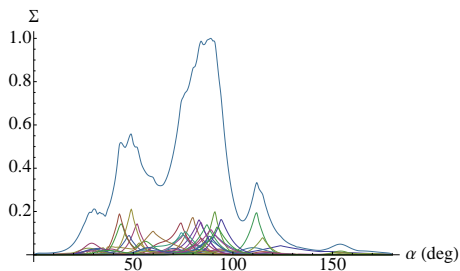
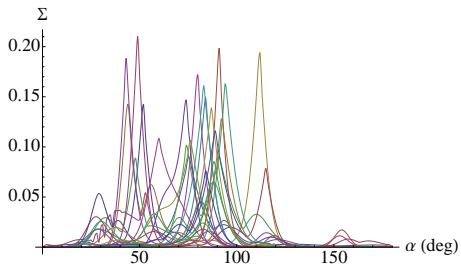
# $\alpha$ SCAN ROBUSTNESS STUDIES V

- Overview of scan results using sum of normalized  $\Sigma$  scans



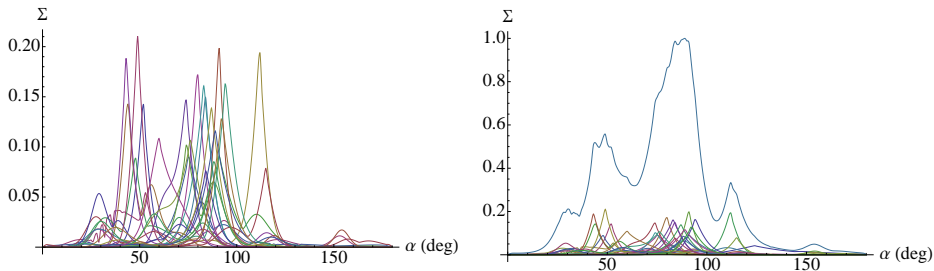
# $\alpha$ SCAN ROBUSTNESS STUDIES V

- Overview of scan results using sum of normalized  $\Sigma$  scans



# $\alpha$ SCAN ROBUSTNESS STUDIES V

- Overview of scan results using sum of normalized  $\Sigma$  scans

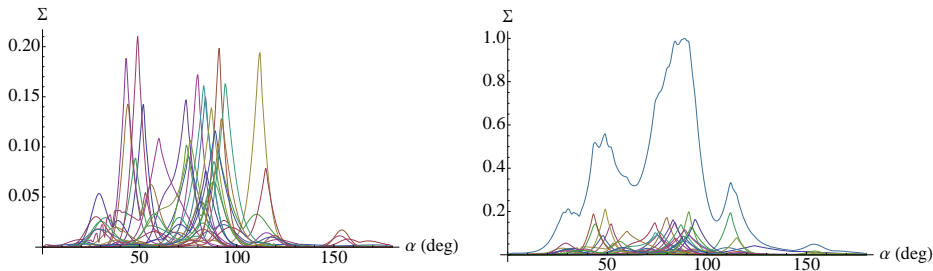


- The study indicates that with the current statistics,  $\alpha$  scans may favor secondary solutions



# $\alpha$ SCAN ROBUSTNESS STUDIES V

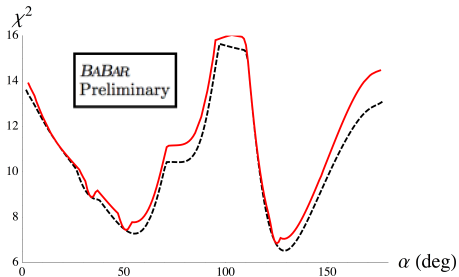
- Overview of scan results using sum of normalized  $\Sigma$  scans



- The study indicates that with the current statistics,  $\alpha$  scans may favor secondary solutions
- When the signal to background ratio is increased, the fit becomes robust

# FINAL FIT $\alpha$ SCAN RESULTS

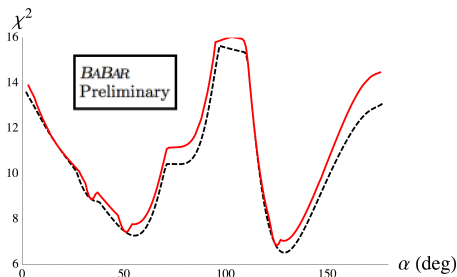
- Due to isospin relations, information about the charged  $B$  decays  $B^\pm \rightarrow \rho^{\pm,0}\pi^{0,\pm}$  may be used to constrain our scan of  $\alpha$
- (Red = isospin constrained scan / Dashed black = new scan from final fit)



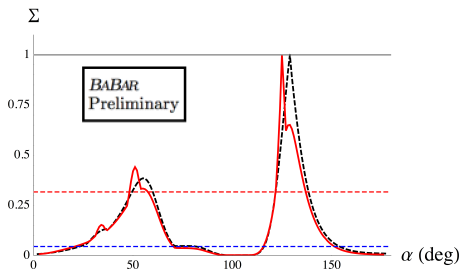
$\alpha$  Scan  $\chi^2$  Distribution

# FINAL FIT $\alpha$ SCAN RESULTS

- Due to isospin relations, information about the charged  $B$  decays  $B^\pm \rightarrow \rho^{\pm,0}\pi^{0,\pm}$  may be used to constrain our scan of  $\alpha$
- (Red = isospin constrained scan / Dashed black = new scan from final fit)



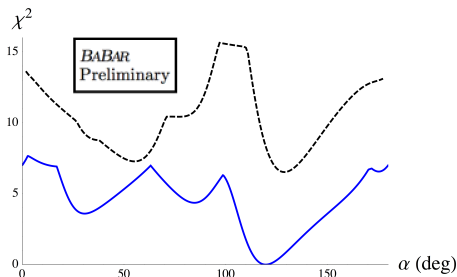
$\alpha$  Scan  $\chi^2$  Distribution



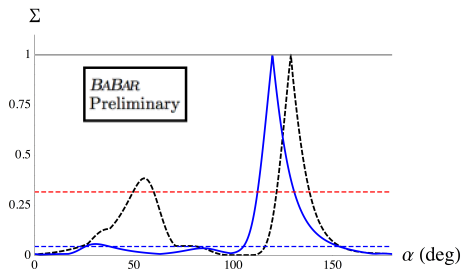
$\alpha$  Scan  $\Sigma$  Distribution

# $\alpha$ SCAN COMPARISON

- Interestingly, though our  $\alpha$  scan disfavors the world average  $\alpha$  value of  $89^\circ$ , it is in good agreement with the existing CKMFitter world average for the  $\rho\pi$  mode
- (Blue = world average / Dashed black = new scan from final fit)



$\alpha$  Scan  $\chi^2$  Distribution



$\alpha$  Scan  $\Sigma$  Distribution

# SUMMARY

- We have performed a time-dependent Dalitz plot analysis of the mode  $B^0 \rightarrow (\rho\pi)^0$  in which we extract 26  $U$  and  $I$  parameter values describing the physics involved

# SUMMARY

- We have performed a time-dependent Dalitz plot analysis of the mode  $B^0 \rightarrow (\rho\pi)^0$  in which we extract 26  $U$  and  $I$  parameter values describing the physics involved
- From these fit results, we extract standard Q2B parameters and find them to be consistent with previously published BaBar and Belle results and robustly extracted

# SUMMARY

- We have performed a time-dependent Dalitz plot analysis of the mode  $B^0 \rightarrow (\rho\pi)^0$  in which we extract 26  $U$  and  $I$  parameter values describing the physics involved
- From these fit results, we extract standard Q2B parameters and find them to be consistent with previously published BaBar and Belle results and robustly extracted
- We also perform a 2D likelihood scan of the direct  $CP$ -violation asymmetry parameters for  $B^0 \rightarrow \rho^\pm \pi^\mp$  decays

# SUMMARY

- We have performed a time-dependent Dalitz plot analysis of the mode  $B^0 \rightarrow (\rho\pi)^0$  in which we extract 26  $U$  and  $I$  parameter values describing the physics involved
- From these fit results, we extract standard Q2B parameters and find them to be consistent with previously published BaBar and Belle results and robustly extracted
- We also perform a 2D likelihood scan of the direct  $CP$ -violation asymmetry parameters for  $B^0 \rightarrow \rho^\pm \pi^\mp$  decays
  - We find the change in  $\chi^2$  between the minimum and the origin (corresponding to no direct  $CP$ -violation) to be  $\Delta\chi^2 = 6.42$ .



# SUMMARY

- We have performed a time-dependent Dalitz plot analysis of the mode  $B^0 \rightarrow (\rho\pi)^0$  in which we extract 26  $U$  and  $I$  parameter values describing the physics involved
- From these fit results, we extract standard Q2B parameters and find them to be consistent with previously published BaBar and Belle results and robustly extracted
- We also perform a 2D likelihood scan of the direct  $CP$ -violation asymmetry parameters for  $B^0 \rightarrow \rho^\pm \pi^\mp$  decays
  - We find the change in  $\chi^2$  between the minimum and the origin (corresponding to no direct  $CP$ -violation) to be  $\Delta\chi^2 = 6.42$ .
- Finally, we perform one-dimensional likelihood-scans of the unitarity triangle angle  $\alpha$  both with and without isospin constraints.

# SUMMARY

- We have performed a time-dependent Dalitz plot analysis of the mode  $B^0 \rightarrow (\rho\pi)^0$  in which we extract 26  $U$  and  $I$  parameter values describing the physics involved
- From these fit results, we extract standard Q2B parameters and find them to be consistent with previously published BaBar and Belle results and robustly extracted
- We also perform a 2D likelihood scan of the direct  $CP$ -violation asymmetry parameters for  $B^0 \rightarrow \rho^\pm \pi^\mp$  decays
  - We find the change in  $\chi^2$  between the minimum and the origin (corresponding to no direct  $CP$ -violation) to be  $\Delta\chi^2 = 6.42$ .
- Finally, we perform one-dimensional likelihood-scans of the unitarity triangle angle  $\alpha$  both with and without isospin constraints.
  - As indicated by our robustness studies, the extraction of  $\alpha$  with our current sample size is not robust.

- We have performed a time-dependent Dalitz plot analysis of the mode  $B^0 \rightarrow (\rho\pi)^0$  in which we extract 26  $U$  and  $I$  parameter values describing the physics involved
- From these fit results, we extract standard Q2B parameters and find them to be consistent with previously published BaBar and Belle results and robustly extracted
- We also perform a 2D likelihood scan of the direct  $CP$ -violation asymmetry parameters for  $B^0 \rightarrow \rho^\pm \pi^\mp$  decays
  - We find the change in  $\chi^2$  between the minimum and the origin (corresponding to no direct  $CP$ -violation) to be  $\Delta\chi^2 = 6.42$ .
- Finally, we perform one-dimensional likelihood-scans of the unitarity triangle angle  $\alpha$  both with and without isospin constraints.
  - As indicated by our robustness studies, the extraction of  $\alpha$  with our current sample size is not robust.
  - Maximum likelihood estimators are known to be Gaussian in general only in the limit of large data sets.

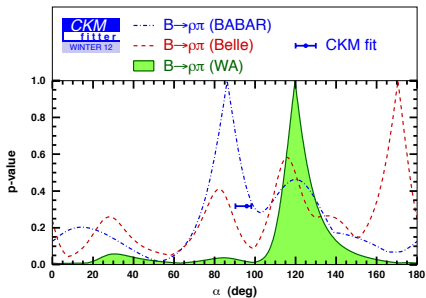
# SUMMARY

- We have performed a time-dependent Dalitz plot analysis of the mode  $B^0 \rightarrow (\rho\pi)^0$  in which we extract 26  $U$  and  $I$  parameter values describing the physics involved
- From these fit results, we extract standard Q2B parameters and find them to be consistent with previously published BaBar and Belle results and robustly extracted
- We also perform a 2D likelihood scan of the direct  $CP$ -violation asymmetry parameters for  $B^0 \rightarrow \rho^\pm \pi^\mp$  decays
  - We find the change in  $\chi^2$  between the minimum and the origin (corresponding to no direct  $CP$ -violation) to be  $\Delta\chi^2 = 6.42$ .
- Finally, we perform one-dimensional likelihood-scans of the unitarity triangle angle  $\alpha$  both with and without isospin constraints.
  - As indicated by our robustness studies, the extraction of  $\alpha$  with our current sample size is not robust.
  - Maximum likelihood estimators are known to be Gaussian in general only in the limit of large data sets.
  - This analysis would benefit greatly from increased sample sizes available at high-luminosity experiments.

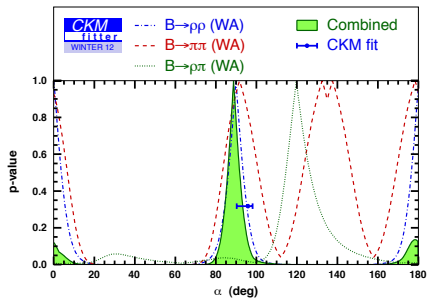
# BACKUP SLIDES

# CKMFITTER $\alpha$ SCANS

- CKMfitter overall world average and  $\rho\pi$  world average  $\alpha$  scans



$\rho\pi$  World Average  $\alpha$  Scan



World Average  $\alpha$  Scan

# $\alpha$ SCAN - ISOSPIN CONSTRAINTS I

- Due to isospin relations, information about the charged  $B$  decays  $B^\pm \rightarrow \rho^{\pm,0}\pi^{0,\pm}$  may be used to constrain our scan of  $\alpha$

# $\alpha$ SCAN - ISOSPIN CONSTRAINTS I

- Due to isospin relations, information about the charged  $B$  decays  $B^\pm \rightarrow \rho^{\pm,0}\pi^{0,\pm}$  may be used to constrain our scan of  $\alpha$
- These relations result in four “constraint” equations while introducing only two new free parameters to the fit (the real and imaginary parts of a tree amplitude,  $T^{+0}$ )



# $\alpha$ SCAN - ISOSPIN CONSTRAINTS I

- Due to isospin relations, information about the charged  $B$  decays  $B^\pm \rightarrow \rho^{\pm,0}\pi^{0,\pm}$  may be used to constrain our scan of  $\alpha$
- These relations result in four “constraint” equations while introducing only two new free parameters to the fit (the real and imaginary parts of a tree amplitude,  $T^{+0}$ )
- The charged  $B$  measurements of interest are the branching fractions and asymmetries:

$$\mathcal{B}(\rho^+\pi^0) = c(|A^{+0}|^2 + |A^{-0}|^2)\tau_{B^+},$$

$$\mathcal{B}(\rho^0\pi^+) = c(|A^{0+}|^2 + |A^{0-}|^2)\tau_{B^+},$$

$$\mathcal{A}(\rho^+\pi^0) = \frac{|A^{-0}|^2 - |A^{+0}|^2}{|A^{-0}|^2 + |A^{+0}|^2},$$

$$\mathcal{A}(\rho^0\pi^+) = \frac{|A^{0-}|^2 - |A^{0+}|^2}{|A^{0-}|^2 + |A^{0+}|^2},$$

where

$$A^{\pm 0} = \frac{q}{p}A(B^\pm \rightarrow \rho^\pm\pi^0),$$

$$A^{0\pm} = \frac{q}{p}A(B^\pm \rightarrow \rho^0\pi^\pm).$$

# $\alpha$ SCAN - ISOSPIN CONSTRAINTS II

- Due to isospin symmetry,

$$\begin{aligned} A^+ + A^- + 2A^0 &= e^{-2i\alpha} (\bar{A}^+ + \bar{A}^- + 2\bar{A}^0) \\ &= \sqrt{2}(A^{+0} + A^{0+}) \\ &= \sqrt{2}e^{-2i\alpha}(A^{-0} + A^{0-}), \end{aligned}$$

$$A^{+0} - A^{0+} - \sqrt{2}(A^+ - A^-) = e^{-2i\alpha} [A^{-0} - A^{0-} - \sqrt{2}(A^- - A^+)].$$

# $\alpha$ SCAN - ISOSPIN CONSTRAINTS II

- Due to isospin symmetry,

$$\begin{aligned}A^+ + A^- + 2A^0 &= e^{-2i\alpha} (\bar{A}^+ + \bar{A}^- + 2\bar{A}^0) \\ &= \sqrt{2}(A^{+0} + A^{0+}) \\ &= \sqrt{2}e^{-2i\alpha}(A^{-0} + A^{0-}),\end{aligned}$$

$$A^{+0} - A^{0+} - \sqrt{2}(A^+ - A^-) = e^{-2i\alpha} [A^{-0} - A^{0-} - \sqrt{2}(A^- - A^+)].$$

- Based on these relations, we can parameterize the charged  $B$  amplitudes according to

$$\begin{aligned}\sqrt{2}A^{+0} &= e^{-i\alpha}T^{+0} + P^+ - P^-, \\ \sqrt{2}A^{0+} &= e^{-i\alpha}(T^+ + T^- + 2T^0 - T^{+0}) - P^+ + P^-, \\ \sqrt{2}A^{-0} &= e^{+i\alpha}T^{+0} + P^+ - P^-, \\ \sqrt{2}A^{0-} &= e^{+i\alpha}(T^+ + T^- + 2T^0 - T^{+0}) - P^+ + P^-. \end{aligned}$$

# $\alpha$ SCAN - ISOSPIN CONSTRAINTS III

- For each of the four amplitudes  $A^{\pm 0}$  and  $A^{0\pm}$ , we can calculate the value based on tree and penguin amplitudes or from measurements of charged  $B$  branching fractions and asymmetries
- Hence, for each of the four amplitudes, we add a gaussian constraint term to the  $\chi^2$  used in the  $\alpha$  scan:

$$\left( \frac{|A_{\text{iter.}|} - |A_{\text{meas.}|}}{\sigma|A_{\text{meas.}|}} \right)^2$$